JOURNAL OF GUIDANCE, CONTROL, AND DYNAMICS
Vol. 16, No. 5, September–October 1993

Longitudinal Dynamics of a Towed Sailplane

Guido de Matteis*
University of Rome "La Sapienza," Rome 00184, Italy

The longitudinal stability of the system represented by towing airplane, cable, and sailplane is investigated. The differential problem concerning the cable dynamics, the boundary conditions of which are the equations of motion of the two planes, is formulated. The resulting set of equations is linearized and the stability analysis is carried out. Strong interactions are shown to take place between cable, tow plane, and sailplane motions, leading to unstable situations in the considered range of practical flight conditions.

Nomenclature

A = rope cross section
C_D, C_L = drag and lift coefficients of the rope
C_{D_0}, k = force coefficients of the rope
C_{M_T} = moment coefficient due to the rope tension
C_T = thrust coefficient
C_W = weight coefficient, $2mg/\rho U_e^2 S$
C_ξ, C_ζ, C_M = aerodynamic coefficients of the planes
c = mean aerodynamic chord
d = rope diameter
E = Young's modulus
F_I, F = inertial and body reference frames
g = acceleration of gravity
I = moment of inertia
$\boldsymbol{L}$ = transformation matrix from F_I to F
l = length of the rope
m = mass
$\boldsymbol{n}$ = vertical unit vector
$\boldsymbol{P}_a$ = position vector of the attachment point
$\boldsymbol{p}$ = unit vector tangent to the rope
q = pitch rate
R = radius of curvature
r = damping coefficient
s = curvilinear abscissa
T = tension
t = time
U, W = velocity components in inertial axes
u, w = velocity components in body axes
V = velocity modulus
$\boldsymbol{v}$ = local velocity vector
x, y, z = coordinates in inertial axes
α = angle of attack
β = flight-path angle
γ = rope mass per unit length
Δz = vertical distance of the planes
δ = elevator angle
ϵ = stretching
θ = pitch angle
λ = eigenvalue
μ = mass density, $2m/\rho Sc$
ξ, η, ζ = coordinates in body axes
ρ = density
σ = real part of the eigenvalue
ω = coefficient of the imaginary part of the eigenvalue

Subscripts

A = tow plane
a = attachment point
B = sailplane
e = equilibrium
G = center of mass
r = relative
0 = unstretched

Superscripts

$'$ = perturbation quantity
$\sim$ = dimensional quantity

I. Introduction

IN this paper we consider the problem of the longitudinal stability of the system represented by towing airplane, cable, and sailplane. The crucial point in approaching the problem is represented by the mathematical modeling of the cable. Whereas the hypothesis of rigid airplane and sailplane is usually made, according to the experimental observations, the description of the flexible cable behavior has to take into account a series of characteristics that can play an important role in establishing the equilibrium of the system as a whole and in determining its dynamics.

After the oldest significant contributions by Bryant et al.,[1] who modeled the tow-cable according to the theories of Hollingdale and Wild,[2] Maryniac, in a series of papers,[3-5] obtained noticeable results when considering both the longitudinal and the transverse stability by assuming that the cable was flexible, elastic, heavy, and subjected to the aerodynamic forces and by neglecting the inertial forces. Lately, DeLaurier[6,7] included these forces in the analysis of the entire system and presented the correct interpretation of a towed flying object as a differential problem concerning the dynamics of an unextensible cable, one of the boundary conditions of which is represented by the equations of motion of the towed body. In this last case, when the possible approximations in dealing with the exact approach of the study are relaxed, namely, small curvature and tension changes along the tracts by which the cable is discretized, the resulting solution procedure involves rather cumbersome calculations. In any case, the dynamics of the tug are not considered.

Recently Cochran et al.[8] investigated the dynamics and control of a maneuverable towed flight vehicle. Again, as in Ref. 6, the end point of the cable that corresponds to the tug proceeds according to a prefixed law, but the rope is inextensible, although its length can change with the time during deployment and retrieval. The interesting study is mainly devoted to control questions.

Presented as Paper 91-2862 at the AIAA Atmospheric Flight Mechanics Conference, New Orleans, LA, Aug. 12-14, 1991; received Oct. 8, 1991; revision received June 28, 1992; accepted for publication Nov. 21, 1992.

*Associate Professor, Department of Mechanics and Aeronautics, via Eudossiana, 18; currently at the Department of Aerospace Engineering, University of Pisa, via Diotisalvi 2, 56126 Pisa. Member AIAA.

Recent advances in computational techniques provide the opportunity for a complete description of the dynamics of the tow plane-cable-sailplane system inclusive of all of the physical characteristics that affect this complicated three-body configuration. This fact, in turn, opens the way to a better understanding of some particular aspects of the three bodies' stability and control, which are of great relevance from the point of view of flight safety. Among the various possible accidents that can happen during towing, see, for example, Ref. 9.

In the author's opinion, the proposed approach appears sufficiently meaningful, general, and correct from a physical point of view since it deals with the complete equations of motion and, as we will see, each component of the system, namely, the two airplanes and the cable, plays a role in the dynamic behavior of the full configuration. In this context, we recall the older, although popular, assumption of a cable treated as being in instantaneous equilibrium, during the motion, with respect to approximate conditions at its ends. This means that the rope's effects on the stability of the vehicles were modeled through certain force conditions at the attachment points.[3,4] Moreover, this formulation led to an ordinary differential system of governing equations. Unfortunately, apart from the criticism regarding the theoretical soundness of such a physical model, sparse and poorly documented data prevented the author from a clear assessment of the grade of accuracy of this simplified, although practical, approach.

The main hypotheses that represent the foundations of the present model are the following. Both the tow plane and the sailplane are rigid bodies; the cable is elastic, although perfectly flexible; the aerodynamic and mass forces on it are taken into account; and the motion of the entire system takes place in a vertical plane.

Furthermore, it is assumed that the initial equilibrium configuration corresponds to a steady flight of the aircraft and the sailplane at constant altitude. The aerodynamic characteristics of the tug and the sailplane are evaluated from reasonable existing experimental data. This is by no means a limitation of the proposed model and the solution procedure when one has in mind the simulation of realistic situations. More detailed representations of the aerodynamic field can be obtained by means of a boundary element method for treating the lifting surfaces, and this would prove useful for investigating some particular problems like the mutual influences of the lifting surface of the tug and the glider or the unsteady wake effects.

The governing equations of the considered system are formulated in Sec. III, and a procedure for the evaluation of the stationary solutions is briefly reported in Sec. V. After linearization of the governing set of equations, the stability and modal analyses are carried out, and their results are reported in Sec. VI. Finally, in Sec. VII, the time history of the system response to a control input on the sailplane is computed and discussed in reference with existing data.

II. Reference Frames and Units

A sketch of the system is given in Fig. 1. Since the fundamental equations for the cable are expressed in an inertial Cartesian system $F_I(x,y,z)$, we will assume that the origin of such a system is initially located in the center of gravity of the tow plane and moves with its initial constant horizontal speed at equilibrium U_e with respect to a flat Earth-fixed inertial frame.

Before proceeding with the presentation of the governing equations, we will say a few words about their nondimensional formulation. Essentially, we have to deal with three sets of equations related to the rope, the tug, and the glider, respectively. It appeared convenient, for the sake of clarity, to use reference units that are natural to each set. For example, when dealing with the lengths, we chose the length of the unloaded cable l_0 and the mean aerodynamic chords of the two planes, c_A and c_B, respectively. Accordingly, the masses of the planes are made nondimensional with respect to $\rho S_A c_A/2$ and $\rho S_B c_B/2$, where S_A and S_B are the wing areas, and the mass per unit length of the rope γ is dimensionless with respect to itself. However, in any case, the reference speed is U_e and the reference time is $c_B/2U_e$. It is understandable how great is the number of characteristic products that are present in the dimensionless equations. From now on all of the quantities are assumed to be nondimensional unless otherwise specified.

As usual, the motion equations of the two planes are formulated in body reference frames $F_A(\xi_A, \eta_A, \zeta_A)$ and $F_B(\xi_B, \eta_B, \zeta_B)$ with origins in the centers of gravity (x_{G_A}, z_{G_A}) and (x_{G_B}, z_{G_B}) and then are transformed into the inertial axes. This choice was made to relate the equations of the planes to the equations of the cable for which they represent the boundary conditions. As a consequence of what has been said before, the aerodynamic forces on the tug and on the towed plane, referred to F_A and F_B, are to be evaluated according to the following expressions of the relative velocity components:

$$u_{r_i} = U_{G_i}\cos\theta_i - W_{G_i}\sin\theta_i + \cos\theta_i$$

$$w_{r_i} = U_{G_i}\sin\theta_i + W_{G_i}\cos\theta_i + \sin\theta_i$$

where $i = A$ and B, θ_i is the pitch angle, u and w are velocity components with respect to F_A and F_B, and U and W refer to F_I.

III. Fundamental Equations

As we said, the approach to the study of the dynamics of the system is based on the dynamics of the cable, which is considered as a continuous, elastic one-dimensional body subjected to distributed mass and aerodynamic forces. The tensions are applied at the ends of the cable, namely, the attachment points of the aircraft and the sailplane. In this respect, the model is analogous to, although much more general than, the one reported in Ref. 10 where the problem of a tethered satellite was considered.

We consider the governing equations of an extensible cable in vector form and express the aerodynamic forces on it as in Ref. 6:

$$\frac{\partial \boldsymbol{v}}{\partial t} = D_D D_S \frac{\partial(\epsilon \boldsymbol{p})}{\partial s} + D_g \boldsymbol{n} + D_A\left[C_D|\boldsymbol{v}_r|\boldsymbol{v}_r + C_L \boldsymbol{v}_r \times (\boldsymbol{v}_r \times \boldsymbol{p})\right] \tag{1}$$

where $\boldsymbol{v} = (U,W)^T$ is the local velocity vector, $\boldsymbol{p} = (\partial x/\partial s, \partial z/\partial s)$ is the unit vector tangent to the rope at the curvilinear abscissa s, and $\boldsymbol{v}_r = -(1+U,W)^T$ is the velocity relative to the air. The stretching ϵ is given by

$$\epsilon = \left[\left(\frac{\partial x}{\partial s_0}\right)^2 + \left(\frac{\partial z}{\partial s_0}\right)^2\right]^{1/2} - 1$$

Furthermore, $D_A = \rho d c_B/4\gamma$, $D_D = c_B/2l_0$, $D_g = g c_B/2U_e^2$, and $D_S = EA/\gamma U_e^2$. For the cable, C_D and C_L are expressed as the ratio of the aerodynamic force components per unit length to $\rho d U_e^2/2$. The scalar expansion of Eq. (1) in F_I gives

$$\frac{\partial U}{\partial t} = D_D D_S \frac{\partial}{\partial s}\left(\epsilon \frac{\partial x}{\partial s}\right) - D_A\left\{C_D\left[(1+U)^2 + W^2\right]^{1/2}(1+U) + C_L\left[W^2\frac{\partial x}{\partial s} - (1+U)W\frac{\partial z}{\partial s}\right]\right\} \tag{2}$$

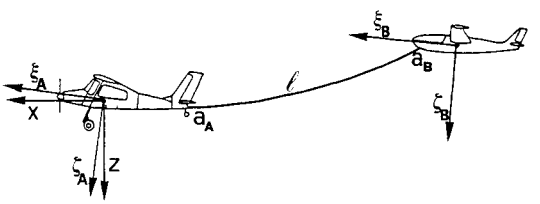

Fig. 1 Sketch of the system.

$$\frac{\partial W}{\partial t} = D_D D_S \frac{\partial}{\partial s}\left(\epsilon \frac{\partial z}{\partial s}\right) + D_g - D_A\left\{C_D\left[(1+U)^2 + W^2\right]^{1/2} W - C_L\left[(1+U)W\frac{\partial x}{\partial s} - (1+U)^2\frac{\partial z}{\partial s}\right]\right\} \tag{3}$$

The following expressions for C_D and C_L were derived, with some manipulations, from Ref. 6:

$$C_D = C_{D_0} + k\left\{1 - \frac{\left[(1+U)\frac{\partial x}{\partial s} + W\frac{\partial z}{\partial s}\right]^2}{(1+U)^2 + W^2}\right\}^{3/2} \tag{4}$$

$$C_L = -k\left\{1 - \frac{\left[(1+U)\frac{\partial x}{\partial s} + W\frac{\partial z}{\partial s}\right]^2}{(1+U)^2 + W^2}\right\} \times \frac{(1+U)\frac{\partial x}{\partial s} + W\frac{\partial z}{\partial s}}{\left[(1+U)^2 + W^2\right]^{1/2}} \tag{5}$$

and the value of the force coefficients C_{D_0} and k can be found in Ref. 11.

At the two ends of the rope, the boundary conditions are supplied, through kinematic relations, by the motion equations of the planes. In writing the governing equations for the aircraft we adopted the classic body-axis form, although with two differences. First, as we said, the inertial terms are written in terms of inertial axis velocity components, and, second, in the force and moment equations, the terms relative to the tension in the cable contain the products $(\epsilon \boldsymbol{Lp})$ and $(\epsilon \boldsymbol{Lp} \times \boldsymbol{P}_a)$, respectively.[12] In particular, at the attachment point of the tug (x_{a_A}, z_{a_A}), we have

$$\frac{dx_{a_A}}{dt} = D_D\left[U_{G_A} - (\xi_{a_A}\sin\theta_A - \zeta_{a_A}\cos\theta_A)q_A/D_C\right]$$
$$\frac{dz_{a_A}}{dt} = D_D\left[W_{G_A} - (\xi_{a_A}\cos\theta_A + \zeta_{a_A}\sin\theta_A)q_A/D_C\right] \tag{6}$$

related to the force equations

$$2\mu_A\left(\cos\theta_A\frac{dU_{G_A}}{dt} - \sin\theta_A\frac{dW_{G_A}}{dt}\right) = D_C C_T - D_C\sin\theta_A C_{W_A} + D_C V_A^2 C_{\xi_A} + D_S D_M D_R D_C \epsilon_{a_A}\left(\frac{\partial x}{\partial s}\bigg|_{a_A}\cos\theta_A - \frac{\partial z}{\partial s}\bigg|_{a_A}\sin\theta_A\right) \tag{7}$$

$$2\mu_A\left(\sin\theta_A\frac{dU_{G_A}}{dt} + \cos\theta_A\frac{dW_{G_A}}{dt}\right) = D_C\cos\theta_A C_{W_A} + D_C V_A^2 C_{\zeta_A} + D_S D_M D_R D_C \epsilon_{a_A} \times \left(\frac{\partial x}{\partial s}\bigg|_{a_A}\sin\theta_A + \frac{\partial z}{\partial s}\bigg|_{a_A}\cos\theta_A\right) \tag{8}$$

and the moment equation

$$I_A\frac{dq_A}{dt} = -\frac{D_S D_M D_R D_C^2}{2}\epsilon_{a_A} \times \left[\xi_{a_A}\left(\frac{\partial x}{\partial s}\bigg|_{a_A}\sin\theta_A + \frac{\partial z}{\partial s}\bigg|_{a_A}\cos\theta_A\right) - \zeta_{a_A}\left(\frac{\partial x}{\partial s}\bigg|_{a_A}\cos\theta_A - \frac{\partial z}{\partial s}\bigg|_{a_A}\sin\theta_A\right)\right] + D_c^2 V_A^2 C_{M_A} \tag{9}$$

where ξ_{a_A} and ζ_{a_A} are the coordinates of the attachment point of the aircraft in body axes; V_A is the relative velocity modulus; $D_C = c_B/c_A$, $D_R = S_B/S_A$; $D_M = 2\gamma/\rho S_B$; and C_ξ, C_ζ, and C_M are the aerodynamic force and moment coefficients in body axes. The meanings of all of the other symbols are standard in flight mechanics (see, for instance, Ref. 12) and appear in the Nomenclature.

Analogously, for the sailplane we write, at the attachment point of the cable (x_{a_B}, z_{a_B}),

$$\frac{dx_{a_B}}{dt} = D_D\left[U_{G_B} - (\xi_{a_B}\sin\theta_B - \zeta_{a_B}\cos\theta_B)q_B\right]$$
$$\frac{dz_{a_B}}{dt} = D_D\left[W_{G_B} - (\xi_{a_B}\cos\theta_B + \zeta_{a_B}\sin\theta_B)q_B\right] \tag{10}$$

and the force and moment equations are

$$2\mu_B\left(\cos\theta_B\frac{dU_{G_B}}{dt} - \sin\theta_B\frac{dW_{G_B}}{dt}\right) = -\sin\theta_B C_{W_B} + V_B^2 C_{\xi_B} - D_S D_M \epsilon_{a_B}\left(\frac{\partial x}{\partial s}\bigg|_{a_B}\cos\theta_B - \frac{\partial z}{\partial s}\bigg|_{a_B}\sin\theta_B\right) \tag{11}$$

$$2\mu_B\left(\sin\theta_B\frac{dU_{G_B}}{dt} + \cos\theta_B\frac{dW_{G_B}}{dt}\right) = \cos\theta_B C_{W_B} + V_B^2 C_{\zeta_B} - D_S D_M \epsilon_{a_B}\left(\frac{\partial x}{\partial s}\bigg|_{a_B}\sin\theta_B + \frac{\partial z}{\partial s}\bigg|_{a_B}\cos\theta_B\right) \tag{12}$$

$$I_B\frac{dq_B}{dt} = \frac{D_S D_M}{2}\epsilon_{a_B}\left[\xi_{a_B}\left(\frac{\partial x}{\partial s}\bigg|_{a_B}\sin\theta_B + \frac{\partial z}{\partial s}\bigg|_{a_B}\cos\theta_B\right) - \zeta_{a_B}\left(\frac{\partial x}{\partial s}\bigg|_{a_B}\cos\theta_B - \frac{\partial z}{\partial s}\bigg|_{a_B}\sin\theta_A\right)\right] + V_B^2 C_{M_B} \tag{13}$$

Furthermore, the following kinematic equations hold:

$$\frac{dx}{dt} = D_D U; \quad \frac{dz}{dt} = D_D W; \quad \frac{d\theta_A}{dt} = q_A; \quad \frac{d\theta_B}{dt} = q_B \tag{14}$$

The pertinent initial conditions are expressed by stating that at $t = 0$, in equilibrium, all of the velocities are zero in F_I, and the coordinates of the points along the cable and at the attachments are

$$x(t=0,s) = x_e(s); \quad z(t=0,s) = z_e(s); \quad x_{a_A}(t=0) = x_{a_{A_e}}$$
$$z_{a_A}(t=0) = z_{a_{A_e}}; \quad x_{a_B}(t=0) = x_{a_{B_e}}; \quad z_{a_B}(t=0) = z_{a_{B_e}} \tag{15}$$

Finally, the pitch angles are

$$\theta_A(t=0) = \theta_{A_e}; \qquad \theta_B(t=0) = \theta_{B_e} \tag{16}$$

IV. Calculation Procedures

All of the calculations for the solution of the partial and ordinary differential equations, corresponding to the various differential problems, were carried out by adopting the differential quadrature method[13] as modified by Satofuka.[14] This solution procedure was demonstrated to be very effective when solving the cable equations.[15]

The computations were performed by assuming for the planes the following characteristic data, i.e., for the tow plane $m_A = 800$ kg, $\bar{I}_A = 1.8 \times 10^3$ kg m^2, $S_A = 16$ m^2, and $c_A = 1.5$ m and for the sailplane $m_B = 300$ kg, $\bar{I}_B = 200$ kg m^2, $S_B = 13$ m^2, and $c_B = 0.94$ m. The aerodynamic data were taken from Refs. 16 and 17. In Eqs. (4) and (5) the coefficients were chosen following Ref. 11, i.e., $C_{D_0} = 0.02$, and $k = 1.15$. In the wide range of variables that can affect the flight conditions, we considered specifically the influence of U_e, $(\xi_{a_{B_e}}, \zeta_{a_{B_e}})$, and the initial vertical position of the glider with respect to the tug

($\Delta z_e = z_{G_{B_e}}$), whereas in all of the calculations the following data were kept constant: $l_0 = 50$ m, $EA = 3.8 \times 10^4$ N, $\gamma = 4 \times 10^{-2}$ kg/m, $\tilde{\xi}_A = -4.9$ m, and $\tilde{\zeta}_A = 0.27$ m.

V. Equilibrium Solution

The initial configuration of the system was calculated by fixing the velocity U_e and the angle of attack of the glider α_{B_e} and then by solving iteratively the equations for the cable and the planes up to the determination of the shape of the rope, the tension at the attachment points, the angle of attack of the tow plane, the control angles δ_{A_e} and δ_{B_e} of the two planes, and, finally, the relative position Δz_e. In Fig. 2 the shape of the cable is presented as a function of the wind speed U_e and the glider angle of attack α_{B_e}. We observe that the geometry of the cable is greatly influenced by U_e and α_{B_e} and, in particular, that the curvature presents relevant variations that affect the perturbed motion of the cable as we will see later.

Let us say a few words on the balance of the forces that act on the rope in determining its shape. We note that at $U_e = 30$ m/s and for α_B such that $\Delta\tilde{z}_e = -28$ m the tension in A is 136 N compared with a value of the total weight, drag, and lift forces on the rope of 20, 60, and 39 N, respectively. Note that the same cable in equilibrium at the same velocity, for $\Delta\tilde{z}_e \simeq 0$, has a tension of 71 N in A, zero lift, and a drag force as low as 4 N.

Figure 3 shows the elevator angles δ_{A_e} and δ_{B_e} and the tension T_{A_e} as functions of the vertical separation $\Delta\tilde{z}_e$ (positive downward) for $U_e = 30$ m/s, being $\tilde{\xi}_B = 1.96$ m and $\tilde{\zeta}_B = 0$. The tension in A, that for small values of $\Delta\tilde{z}_e$ balances the sailplane and cable drag, increases exponentially for a larger vertical distance between the planes. The figure shows that for the considered range of relative positions the control angles are within reasonable limits.

As for the static stability of the sailplane, the derivative[3] $d(C_{M_B} + C_{M_T})/dC_{\zeta_B}$ is equal to 2.4 for $U_e = 30$ m/s and $\tilde{\xi}_B = 1.96$ m, the value being nearly constant as α_B is varied. The static margin of the glider in free flight is 0.34 so that this parameter is increased by the towing action, at least for a forward position of the attachment point with respect to the center of gravity.

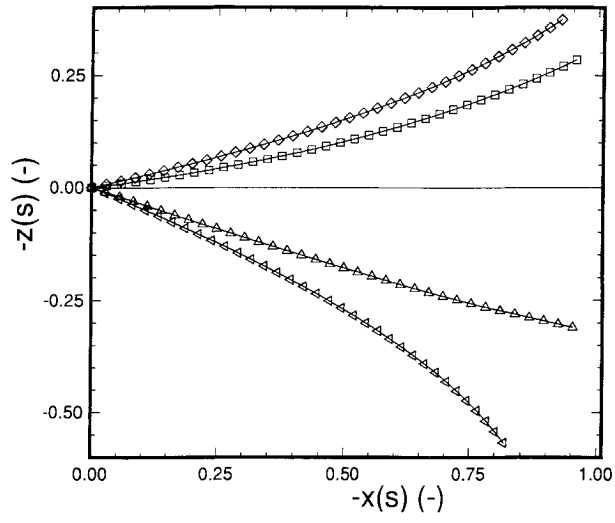

Fig. 2 Shape of the cable: ◇, $U_e = 50$ m/s, $\alpha_{B_e} = 1.9$ deg; □, $U_e = 30$ m/s, $\alpha_{B_e} = 4.9$ deg; Δ, $U_e = 30$ m/s, $\alpha_{B_e} = 1.9$ deg; ◁, $U_e = 50$ m/s, $\alpha_{B_e} = 1.7$ deg.

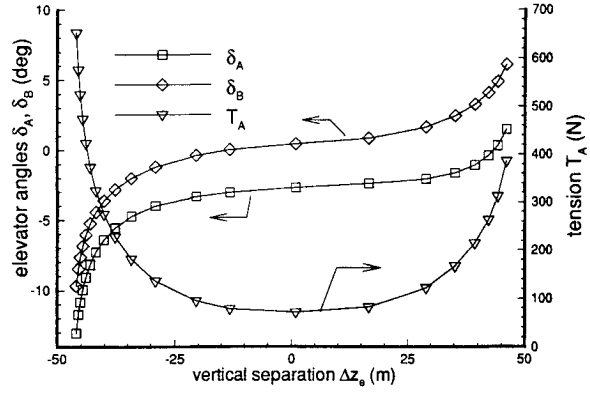

Fig. 3 Elevator angles δ_{A_e} and δ_{B_e} and tension T_A vs vertical separation of the planes $\Delta\tilde{z}_e$: $U_e = 30$ m/s.

VI. Stability Analysis

We applied the usual linearization method to the basic equations to determine the stability characteristics of the system. One should keep in mind that the linearization process of the aerodynamic terms is carried out with reference to the body-fixed frames F_A and F_B, which are not stability frames. Therefore, the derivatives of the aerodynamic force coefficients are to be correctly interpreted.

The set of linearized equations can be put in a discretized form following the method in Sec. IV and leads to

$$F\dot{X} = GX \tag{17}$$

where the state vector is

$$X^T = \left(U'_{G_A}, U'_2, \ldots, U'_{N-1}, U'_{G_B}, W'_{G_A}, W'_2, \ldots, W'_{N-1}, W'_{G_B}, x'_1, \ldots, x'_N, z'_1, \ldots, z'_N, q'_A, q'_B, \theta'_A, \theta'_B\right)$$

The apex indicates perturbation variables and the subscript $i = 1, \ldots, N$ affects the value in the ith node. Equation (17), after normalization, yields $\dot{X} = AX$ with $A = F^{-1}G$. Standard methods supply the eigenvalue and eigenvectors of the $4(N+1) \times 4(N+1)$ matrix A. A number of nodes N equal to 50 were used in the calculations.

The dynamics of the cable were analyzed first. In this respect, the solution to the eigenproblem (17) yields the classical result of transverse and longitudinal vibration modes. The frequency of the longitudinal modes is in fair agreement with the expression $\omega_{l_n} = n\pi\sqrt{EA/\gamma l^2}$ where n is the mode number. When the transverse modes are dealt with, reference is to be made to the parameter $K^2 = l^2 EA/TR^2$ where R is the radius of curvature of the rope in equilibrium. The critical value $K_c = 2\pi$ indicates whether the rope behaves extensibly ($K < K_c$) or inextensibly ($K > K_c$).[18,19] In the latter case, Irvine and Caughey[18] demonstrated that, for a pinned-pinned elastic catenary, the frequency of the first symmetric mode is larger than the frequency of the first antisymmetric mode. Perhaps it is more interesting to recall that Von Flotow and Wereley[19] showed that, in the same situation, strong coupling between the first longitudinal and transverse modes can take place.

Typical values of the parameter K in the present case are in the region of the critical value, K being larger for smaller $|\Delta z_e|$ due to the relatively low tension. In particular, Fig. 4 reports the coefficient of the imaginary part of the eigenvalue $\tilde{\omega}$ and the mode shape of the first four transverse vibrational modes calculated for $U_e = 30$ m/s and $\Delta\tilde{z}_e = 1.1$ m. It results in $K \simeq 7$, and the behavior predicted in Ref. 18 is confirmed. A final observation concerns the damping coefficient r of the elastic modes that significantly increases with the distance between the two planes due to more intense aerodynamic actions on the cable. For instance, it is $r = 9 \times 10^{-3}$ for $\Delta\tilde{z}_e = 1.1$ m and $r = 0.2$ for $\Delta\tilde{z}_e = 42$ m.

Coming now to the dynamic stability of the planes, we observe that the short period (SP) modes are practically unaffected by the towing, i.e., for $U_e = 30$ m/s and $\Delta\tilde{z}_e = 1.1$ m, the pertinent eigenvalues are $\tilde{\lambda}_{SP_A} = -2.01 \pm 2.47i$ rad/s and

Table 1 Eigenvalues and eigenvectors of the first four modes: $U_e = 30$ m/s, $\alpha_B = 4.6$ deg

			Mode			
	PH_A	PH_B	1	2	3	4
$\bar{\lambda}$	$-1.7(-2)\pm 3.6(-1)i$	$-8.0(-3)\pm 3.6(-1)i$	$1.6(-1)$	$9.3(-3)$	$-3.0(-2)\pm 3.7(-1)i$	$-1.5(-1)\pm 8.5(-1)i$
V_A	$8.3(-3)\pm 4.6(-2)i$	0	$6.6(-2)$	$4.2(-3)$	$9.4(-2)\pm 1.0(-2)i$	$-2.0(-2)\pm 3.6(-2)i$
V_B	0	$5.3(-3)\pm 4.6(-2)i$	$5.6(-2)$	$4.2(-3)$	$9.7(-2)\pm 1.1(-2)i$	$4.7(-2)\pm 1.6(-2)i$
α_A	$-1.1(-3)\pm 7.6(-3)i$	0	$-2.1(-2)$	$-1.2(-3)$	$-1.5(-2)\pm 2.4(-4)i$	$-1.2(-3)\pm 8.6(-3)i$
α_B	0	$-1.7(-4)\pm 1.3(-3)i$	$-2.6(-3)$	$-2.6(-4)$	$-2.8(-3)\pm 5.2(-5)i$	$-1.1(-3)\pm 9.9(-4)i$
q_A	$-1.0(-5)\pm 1.5(-4)i$	0	$-1.1(-4)$	$-1.3(-7)$	$3.2(-4)\pm 2.1(-5)i$	$-6.7(-5)\pm 3.5(-3)i$
q_B	0	$2.4(-5)\pm 1.5(-4)i$	$7.0(-5)$	$6.9(-8)$	$3.0(-4)\pm 5.2(-5)i$	$1.6(-4)\pm 2.3(-5)i$
θ_A	$-2.7(-2)\pm 3.0(-3)i$	0	$4.2(-2)$	$9.0(-4)$	$-8.1(-3)\pm 5.5(-2)i$	$-2.4(-2)\pm 9.3(-3)i$
θ_B	0	$2.6(-2)\pm 4.7(-3)i$	$2.7(-2)$	$4.7(-4)$	$4.9(-3)\pm 5.2(-2)i$	$-3.7(-3)\pm 1.1(-2)i$

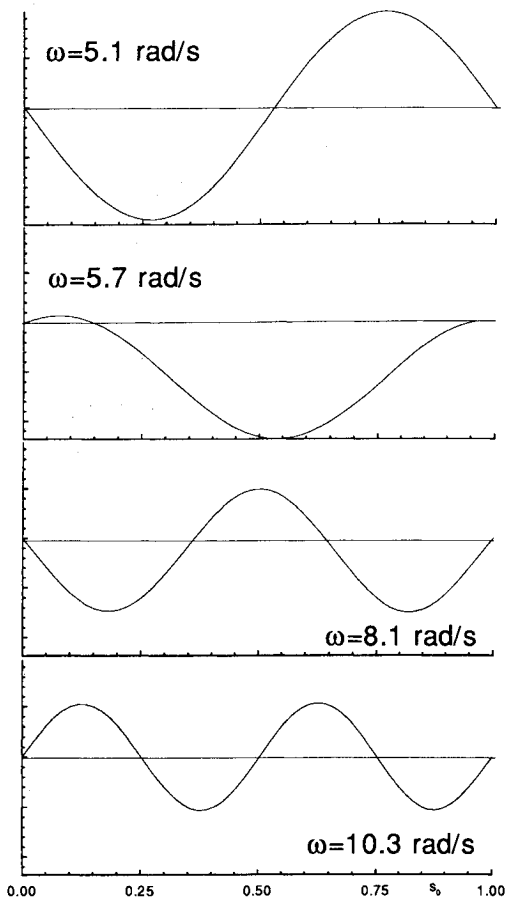

Fig. 4 Shapes of the first four transverse modes: $U_e = 30$ m/s, $\Delta\tilde{z}_e = 1.1$ m.

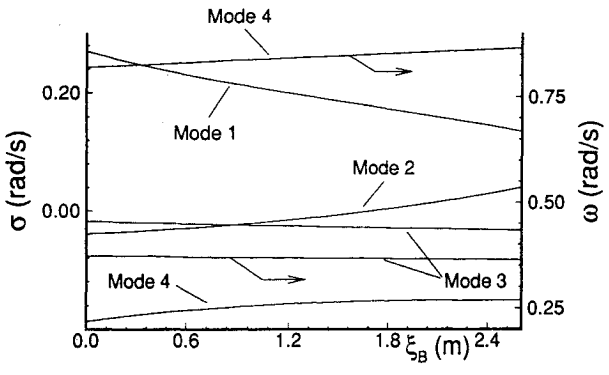

Fig. 5 Real part $\tilde{\sigma}$ and coefficient of the imaginary part $\tilde{\omega}$ of the eigenvalues of modes 1-4 vs $\tilde{\xi}_{a_B}$: $U_e = 30$ m/s, $\alpha_{B_e} = 4.6$ deg, $\tilde{\zeta}_{a_B} = 0$.

$\bar{\lambda}_{SP_B} = -7.20 \pm 7.03i$ rad/s for the free planes and $\bar{\lambda}_{SP_A} = -1.97 \pm 2.50i$ rad/s and $\bar{\lambda}_{SP_B} = -7.30 \pm 7.09i$ rad/s in towed flight. On the other hand, an intense interaction between the tug, the sailplane, and the cable motion takes place at lower frequencies. This is evident when Table 1 is considered. There the eigenvalues and the corresponding eigenvectors are shown relative to the state variables of the planes as calculated 1) for the planes in free flight (PH_A and PH_B) and 2) for the first four modes of the entire system, the flight parameters being those reported earlier. We see that two aperiodic (modes 1 and 2) and two periodic (modes 3 and 4) modes are present in accordance with the results of Refs. 3 and 4. The reported components of the eigenvectors show that the four modes involve excitation of the state variables of both the tug and the glider to such an extent that separate PH are not recognizable.

Mode 1 corresponds to a rapidly diverging motion (the time constant is 6.1 s) where the velocity of the two vehicles increases and the flight-path angle $\beta = \theta - \alpha$ is decreasing for the tow plane ($\beta = -2.1 \times 10^{-2}$) and growing for the sailplane ($\beta = 3.0 \times 10^{-2}$). This appears to correspond to the unsafe situation described in Ref. 9 where the sequence of events sees the glider achieve a higher position behind the tug and the tug pitch sharply nose downward while the speeds of the two vehicles significantly increase. In fatal accidents, this glider/towplane upset is reported to happen so rapidly that the tug pilot is unable to release.

As an application of the present formulation, the effects of the attachment point and the relative position of the planes on the system stability are discussed in the following figures. In particular, Fig. 5 shows the real part $\tilde{\sigma}$ and the coefficient of the imaginary part $\tilde{\omega}$ of the eigenvalues of modes 1-4 as a function of $\tilde{\xi}_{a_B}$ for $\tilde{\zeta}_{a_B} = 0$. The periodic modes are slightly affected by this parameter, whereas $\tilde{\sigma}$ decreases for mode 1 and grows for mode 2 as the attachment point moves forward so that, for $\tilde{\xi}_{a_B} > 1.2$ m, the second aperiodic mode is also divergent.

The eigenvalues of the same modes are reported in Fig. 6 vs $\tilde{\zeta}_{a_B}$ for $\tilde{\xi}_{a_B} = 2$ m. As far as mode 1 is concerned, we see a stronger divergence for an attachment point of the rope below the center of gravity and an opposite effect when $\tilde{\zeta}_{a_B}$ is negative. This result can be explained by considering the effect of the moment due to the tension, which is positive (nose up) for $\tilde{\zeta}_{a_B} > 0$ and negative (nose down) for $\tilde{\zeta}_{a_B} < 0$. Mode 3 is not affected by $\tilde{\zeta}_{a_B}$, and the damping of mode 4 is always increasing with $\tilde{\zeta}_{a_B}$. For $\tilde{\zeta}_{a_B} < 0.3$ m, modes 1 and 2 meet to form a third oscillatory mode.

Finally, Fig. 7 shows the effect of the relative vertical position at equilibrium $\Delta\tilde{z}_e$ of the two vehicles on the same modes. We note a quite complex behavior of the four considered eigenvalues. However, a positive effect is apparent when the glider is flying below the tug, even though, for $\Delta\tilde{z}_e > 25$ m, mode 4 rapidly diverges. This result appears to confirm, at least qualitatively, the conclusions in Ref. 3, which were obtained by a much simpler model, where a position of the sailplane below the tow plane is reported to increase the stability. Moreover, we observe that the second periodic mode (dashed line) is nearly undamped, that modes 1 and 2 form a periodic

root for $\Delta\tilde{z}_e > 24$ m that again splits off into two real roots for $\Delta\tilde{z}_e > 40$ m, and that mode 4 is aperiodic for $\Delta\tilde{z}_e < -30$ m.

A few cases were run at $\alpha_B = 4.6$ deg to analyze the effects of the length of the rope and of the aerodynamic forces acting on it. In the first situation, l_0 influences the vibrational frequencies of the cable as expected. The slight variation observed in the eigenvalues of modes 1 and 2 can be ascribed to the variation of the total mass of the rope and, consequently, of Δz following a variation of l_0 for α_B and γ kept constant. As for the influence of the aerodynamic forces on the rope on the overall system stability, we find that they are responsible for the damping of the vibrational modes of the rope. Furthermore, when these actions are neglected by setting $k = C_{D_0} = 0$ in Eqs. (4) and (5), then we observe a 3% decrease in the eigenvalue of mode 1. This last result is probably related to a slightly different shape of the cable at equilibrium in the considered case.

An important and final point concerns the interaction of the cable dynamics with the vehicles. In other words, are the cable mass and its internal dynamics relevant in the stability analysis

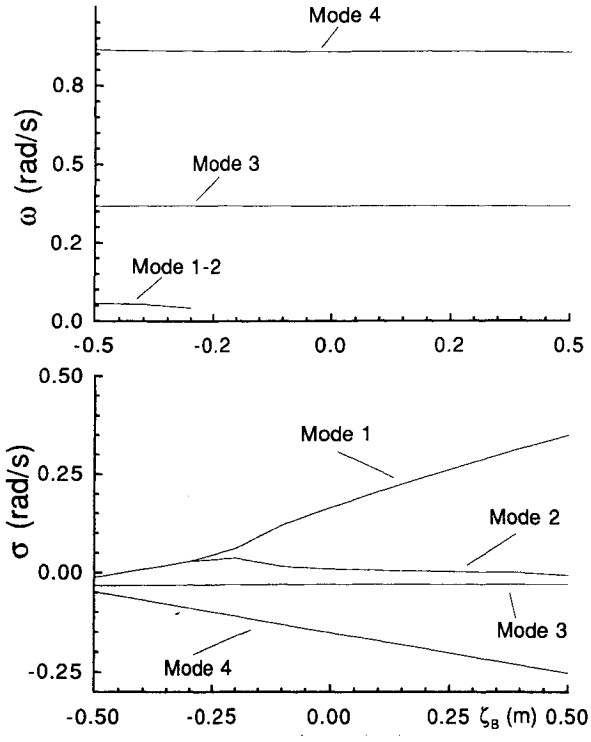

Fig. 6 Real part $\tilde{\sigma}$ and coefficient of the imaginary part $\tilde{\omega}$ of the eigenvalues of modes 1-4 vs $\tilde{\zeta}_{a_B}$: $U_e = 30$ m/s, $\alpha_{B_e} = 4.6$ deg, $\tilde{\xi}_{a_B} = 2$ m.

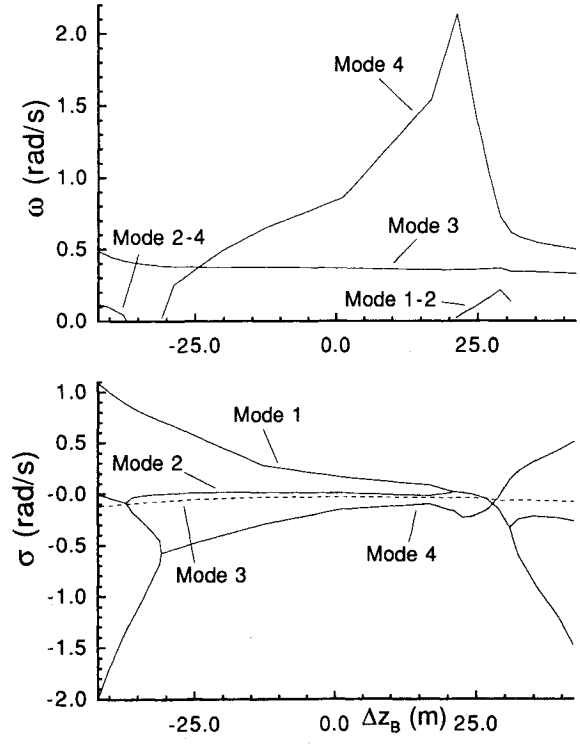

Fig. 7 Real part $\tilde{\sigma}$ and coefficient of the imaginary part $\tilde{\omega}$ of the eigenvalues of modes 1-4 vs $\Delta\tilde{z}_e$: $U_e = 30$ m/s, $\tilde{\xi}_{a_B} = 2$ m, $\tilde{\zeta}_{a_B} = 0$.

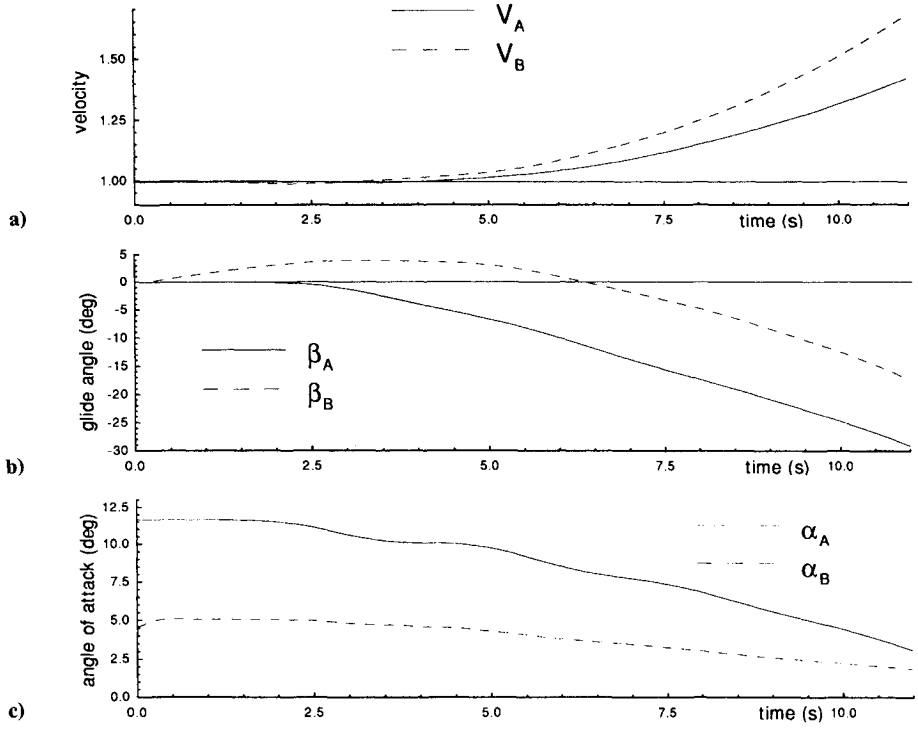

Fig. 8 Response to elevator, $\Delta\delta_B = -1$ deg, $U_e = 30$ m/s: a) velocity module, b) flight-path angle, and c) angle of attack.

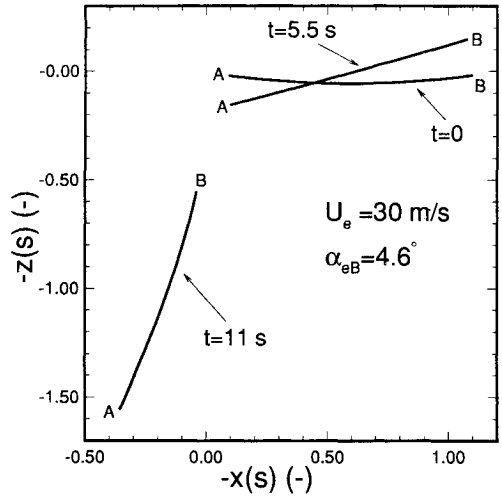

Fig. 9 Cable shape and position at different times, $\Delta\delta_B = -1$ deg, $U_e = 30$ m/s.

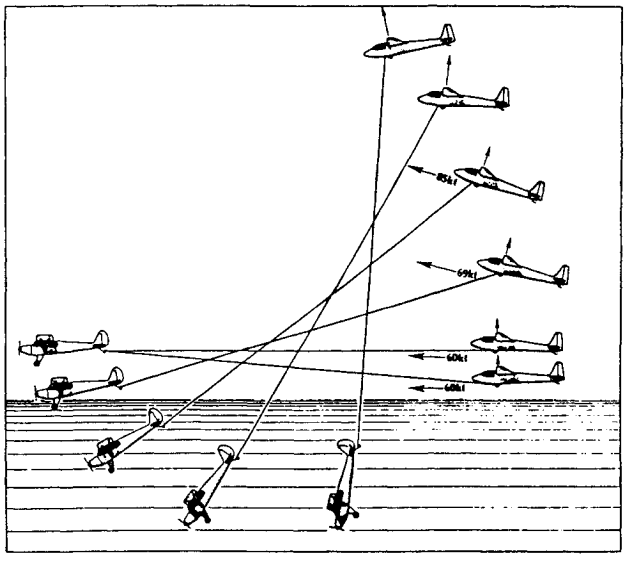

Fig. 10 Sequence of events during a glider/tow plane upset.[9]

of the system? The frequency of the cable vibrations is quite high (above 5 rad/s) compared with the slow phugoid and aperiodic modes. However, as pointed out in Ref. 19, the elastic modulus, the tension, and the curvature are all important in determining the dynamics of the complete system. As a test, we observe that, as the mass of the cable is reduced and the vertical separation is small, the cable configuration approaches that of a straight line and the frequency of mode 4 tends to the elastic oscillation (bounce) value,[19] i.e., $\tilde{\omega}_4 = 1.8$ rad/s, which is rather different from the actual value of 8.8×10^{-1} rad/s.

VII. Nonlinear Simulation

The full set of nonlinear equations of motion for the three bodies [Eqs. (2-14)] was integrated in time by a fourth-order Runge-Kutta method. The same technique reported in Sec. IV was used for the space discretization of the cable equations (2-5) for a number of nodes $N = 35$ and the time step was $\Delta\tilde{t} = 1.4 \times 10^{-3}$ s. The initial conditions for the state variables were those reported in Eqs. (15) and (16), and the response to a step input $\Delta\delta_B = -1$ deg of the glider elevator was evaluated.

Figures 8a-8c report the time histories of V, β, and α for the tug (A) and the glider (B), the reference flight parameters being $U_e = 30$ m/s, $\alpha_{B_e} = 4.6$ deg, $\tilde{\xi}_B = 1.2$ m, and $\tilde{\zeta}_B = 0$. The eigenanalysis of the linearized problem corresponding to this situation is that in Table 1. In Fig. 8a we observe an exponential increase in the velocities, that of the sailplane being higher due to its pendular motion about the tug. Figure 8b shows that the sailplane initially climbs up, acquiring a higher position with respect to the tow plane, and after a few seconds begins to pitch down, whereas the tug after 2.5 s is already pitching down due to the negative moment caused by the cable tension. In Fig. 8c we see that α_B, which is initially increased by the control action, then steadily decreases for $\tilde{t} > 3$ s, whereas α_A is significantly decreasing from the beginning of the maneuver.

Figure 9 shows the shape and the position of the cable at three different times, i.e., $\tilde{t} = 0$, 5.5, and 11 s in the same situation and we note the upward initial displacement of the sailplane. After 11 s, the cable configuration is nearly vertical, and the two planes are both rapidly losing altitude. It is worth recalling that the reference frame is moving at $U_e = 30$ m/s with respect to the Earth-fixed frame. For comparison, in Fig. 10 we report from Ref. 9 the sequence of events occurring during the glider/tow-plane upset as already discussed in Sec. VI. The numerical results confirm the insurgence and development of that sequence.

VIII. Conclusions

The objective of this study was to analyze the three-body system represented by a towed sailplane. The proposed formulation is complete in the sense that it accounts for the motions of tug and glider and for the cable dynamics. The linearized set of governing partial and ordinary differential equations is discretized, and modal and stability analyses are carried out.

The resulting values of the cable curvature and tension for standard values of the system parameters and usual flight conditions are such that the cable vibrations follow either an extensible or an inextensible behavior that adds some complexity to the analysis, related to possible mode interactions in the latter situation.

The stability analysis shows that the short period modes of the two vehicles are slightly affected by the towing, whereas the phugoid modes present a strong coupling with the dynamics of the cable. A lower position of the sailplane with respect to the tug, together with the attachment point in an upper position relative to the glider's center of gravity, has a positive effect on the system's stability.

A divergent aperiodic mode is shown to correspond to the observed instability of the system that in the past caused a number of accidents.

As a final conclusion, the proposed model can lend itself to a wide range of applications whenever a rigorous and complete solution of the cable-body problem is required.

References

[1]Bryant, L. W., Brown, W. S., and Sweeting, N. E., "Collected Researches on the Stability of Kites and Towed Gliders," *Aeronautical Research Council,* R. & M. 2303, London, England, UK, Feb. 1942.

[2]Hollingdale, S. H., and Wild, N. E., "The Effect of Wind on the Configuration of the Flying Cable of a Kite Balloon," Royal Aircraft Establishment, Rept. D.I./67, 1937.

[3]Maryniac, J., "Simplified Longitudinal Stability of a Towed Sailplane," *Mechanica Teoretyczna i Stozowana,* Vol. 5, No. 1, 1967, pp. 57-101.

[4]Maryniac, J., "Dynamic Longitudinal Stability of a Towed Sailplane," *Mechanica Teoretyczna i Stozowana,* Vol. 5, No. 3, 1967, pp. 347-383.

[5]Maryniac, J., "Dynamic Lateral Stability of a Towed Glider in Steady Horizontal Flight," *Aero-Revue,* No. 2, 1970, pp. 86-89.

[6]De Laurier, J. D., "A First Order Theory for Predicting the Stability of Cable Towed and Tethered Bodies Where the Cable Has a General Curvature and Tension Variation," von Kármán Inst., TN 68, Rhode-Saint-Genese, Belgium, Dec. 1970.

[7]De Laurier, J. D., "A Stability Analysis for Tethered Aerodynamically Shaped Baloons," *Journal of Aircraft,* Vol. 9, No. 9, 1972, pp. 646-651.

[8]Cochran, J. E., Innocenti, M., No, T. S., and Thukral, A., "Dy-

namics and Control of Maneuverable Towed Flight Vehicles," AIAA Paper 90-2841-CP, 1990.

[9]Irving, F., "Glider/Tow-Plane Upsets," *Aero-Revue,* No. 6, 1986, pp. 39–43.

[10]de Matteis, G., and de Socio, L. M., "Dynamics of a Tethered Satellite Subjected to Aerodynamic Forces," *Journal of Guidance, Control, and Dynamics,* Vol. 14, No. 6, 1991, pp. 1129–1135.

[11]Hörner, S. F., *Fluid Dynamic Drag,* Hoerner, Midland Park, NJ, 1958.

[12]Etkin, B., *Dynamics of Atmospheric Flight,* Wiley, New York, 1972.

[13]Bellman, R., and Adomian, G., *Partial Differential Equations,* D. Reidel Pub. Co., Dordrecht, The Netherlands, 1984.

[14]Satofuka, N., "A New Explicit Method for the Numerical Solution of Parabolic Differential Equations," *Numerical Properties and Methodologies in Heat Transfer,* edited by T. M. Shih, Hemisphere, Washington, DC, 1983, pp. 97–108.

[15]de Matteis, G., and de Socio, L. M., "A Discretized Model for the Dynamics of a Tethered Satellite System and Applications," *Mathematical Models and Methods in Applied Sciences,* Vol. 1, Sept. 1991, pp. 377–398.

[16]Morelli, P., *Static Stability and Control of Sailplanes,* Organisation Scientifique et Technique Internationale du Vol à Voile, Voorburg, The Netherlands, 1976.

[17]Smetana, F. O., *Computer Assisted Analysis of Aircraft Performance Stability and Control,* McGraw-Hill, New York, 1984.

[18]Irvine, H. M., and Caughey, T. K., "The Linear Theory of the Free Vibrations of a Suspended Cable," *Proceedings of the Royal Society of London,* Series A, Vol. 341, 1974, pp. 299–315.

[19]Von Flotow, A. H., and Wereley, N. M., "Insight and Approximations in Dynamic Analysis of Spacecraft Tethers," *Mechanics and Control of Large Space Structures,* edited by J. L. Junkins, Progress in Astronautics and Aeronautics, AIAA, Washington, DC, 1990, pp. 667–696.